**Solid Freeform Fabrication 2021: Proceedings of the 32nd Annual International Solid Freeform Fabrication Symposium – An Additive Manufacturing Conference**
**Reviewed Paper**

# Applied Viscous Thread Instability for Manufacturing 3D Printed Foams

B. Emery[1], D. L. Revier[2,3], J. I. Lipton[2,3]

1. Department of Physics, University of Washington, Seattle, Washington 98195, USA
2. Paul G. Allen School of Computer Science & Engineering, University of Washington, Seattle, Washington 98195, USA
3. Department of Mechanical Engineering, University of Washington, Seattle, 98195, USA

## Abstract

Traditional foams are fabricated via stochastic chemical processes that yield homogeneous material properties. Foams can exhibit a wide range of material properties by varying process controls allowing them to be used in many industrial and commercial applications. Previously, additive manufacturing could only produce foam approximations in the form of traditional lattice infill. Our work employs viscous thread printing (VTP) of thermoplastic polyurethane (TPU) on a fused filament fabrication (FFF) printer, exploiting the semi-viscous nature of extruded filament to coil producing a new type of printed foam. Specimens were tested under compression to determine uniformity along principal axes and behavior under strain when compared to infill patterns, such as grid and cubic. This work establishes that VTP as applied to TPU can be used to manufacture programmable stiffness foams as a function of density, suited to a variety of needs and should be considered as an alternative to traditional foams and other printed lattice geometries.

**Keywords:** Foams, Viscous Thread Instability, Viscous Thread Printing, Cellular Structures

## Introduction

Additive manufacturing (AM) processes, also called "3D printing", are commonly used to fabricate porous cellular structures for a variety of applications from bio-printing for cellular scaffolding and medical implants [1,2] to mechanical applications for weight reduction as well as optimizing static and dynamic mechanical properties [3]. Traditionally, printed cellular structures are fabricated in one of two ways: 1) explicitly defining the geometry though design of the cells themselves or 2) implicitly through tool path processing such as volume-filling paths commonly called "infills."

The explicit definition of cellular structures requires printer resolution to be much finer than that of the cellular structure unit cell, usually by at least one order of magnitude or more [3–6]. Furthermore, these geometries require design of complex cellular structures though defined cellular structures such as octet truss unit cells or through topology optimization [7–9], in which the design space is tightly bounded or arbitrarily large respectively. Ultimately, cell size and design are significant limitations to an explicitly defined cellular geometry for printed objects.

Conversely, implicit cellular structure definition (i.e. an infill algorithm) is not sufficient for engineered materials because they often rely on "black box" algorithms, are geometric in

nature, and tend to be anisotropic [10]. Infills with back-and-forth toolpath patterns such as "grid" or more sophisticated geometric definitions such as "cubic" can only be reasonably controlled through one variable, the infill percentage, and furthermore must remain consistent or rely on discrete "steps" to incrementally increase density throughout the geometry, disallowing any possibility of material property gradients. Ultimately, implicit cellular definition algorithms are adequate in many simple use cases, but are insufficient from an engineered materials perspective.

In this work we extend a printing technique known as Viscous Thread Printing (VTP) [11] for use with thermoplastic polyurethane (TPU) on a common Fused Filament Fabrication (FFF) printers. We generate cellular foam structures at resolutions that are comparable to the native resolution of the printer by utilizing the phenomenon of Viscous Thread Instability (VTI). VTI is a well characterized phenomenon in 1D and 2D [12–15] that is familiar to anyone who has seen honey cascade from a spoon onto toast. The bending and coiling pattern that the viscous fluid makes as the thread traverses the surface is simple, yet well-controlled phenomenon in 1D. Extending to 2D and 3D, VTI becomes much less predictable or controllable; however, can still result in a wide variety of coiling patterns classified into shapes such as W's, meanders, alternating loops and translating coils [13,15] which can be exploited to generate 3D structures when stacked.

In this paper we demonstrate that VTP of TPU results in an implicitly defined, open-celled, foam structure with uniform stiffness along principal axes. We focus on translating and alternating coils since they produce the greatest number of interconnections between strands. We show that by manipulating simple print parameters we can print single-layer, non-woven textiles on a standard FFF 3D printer. When stacked layer upon layer the results are 3D open-celled foams with programmable stiffness as a function of density that can vary over multiple orders of magnitude.

## TPU VTP Process Characterization

TPU behaves as a viscous liquid in its semi-molten state when printed using an extrusion-based process such as FFF. The key parameters to determine the coiling behavior of the TPU are the dimensionless velocity variable V* and the dimensionless height variable H*,

$$V^* = \frac{F}{C}$$

$$H^* = \frac{H}{\alpha D}$$

where F is the linear translation speed of the printhead, C is the linear velocity of the material being extruded, H is the print height, D is the nozzle diameter and α is die swell, a material and process dependent constant. Each of these variables can be controlled either explicitly or implicitly directly through g-code commands. Together, the V*,H* combination have a dominant effect in determining the type of coiling behavior exhibited as well as the spatial frequency of the coiling respectively [12,13,15].

There are two main regimes of coiling that are of interest for VTP foams: translating coiling and alternating coiling. Translating coiling results from a specific combination of V*,H* to produce a continuous path of overlapping loops of material. Translating coiling is most interesting because it allows for the greatest number of interconnections of a single thread producing a structure that is porous and homogenous in macro structure. Alternating coiling may be used for

VTP foams but is less desired because it produces fewer interconnections and is, in general, a less regular structure. Finally, one other significant regime is accumulation (i.e. over-extrusion). Accumulation is not desired because the thin nature of the thread is lost and instead produces solid structures more similar to conventional FFF parts than foams [15].

### 1D/2D Characterization

First, we established preliminary bounds on V*/H* for TPU by printing spreads of 1D lines to establish the range of coiling behaviors and frequencies able to be produced as shown in **Figure 1**. Initial tests were performed using already established V*/H* bounds for prior work on similar materials [11] and then were expanded to test full theoretical bounds for varying coiling instability domains. We determined for TPU that V* within the range of 0.12-1.0 and H* >5 for 1D lines produced the variety of coiling behaviors and densities that would allow for control of foam density. For V* < 0.12 we observed over-extrusion, also called accumulation, that would have required unrealistic amounts of filament to be extruded, resulting in a lack of any significant coiling. For V* > 1 no coiling behavior was observed and the TPU had difficulty sticking to the build plate in many cases. For H* < 5 we observed a very high coiling frequency bordering on

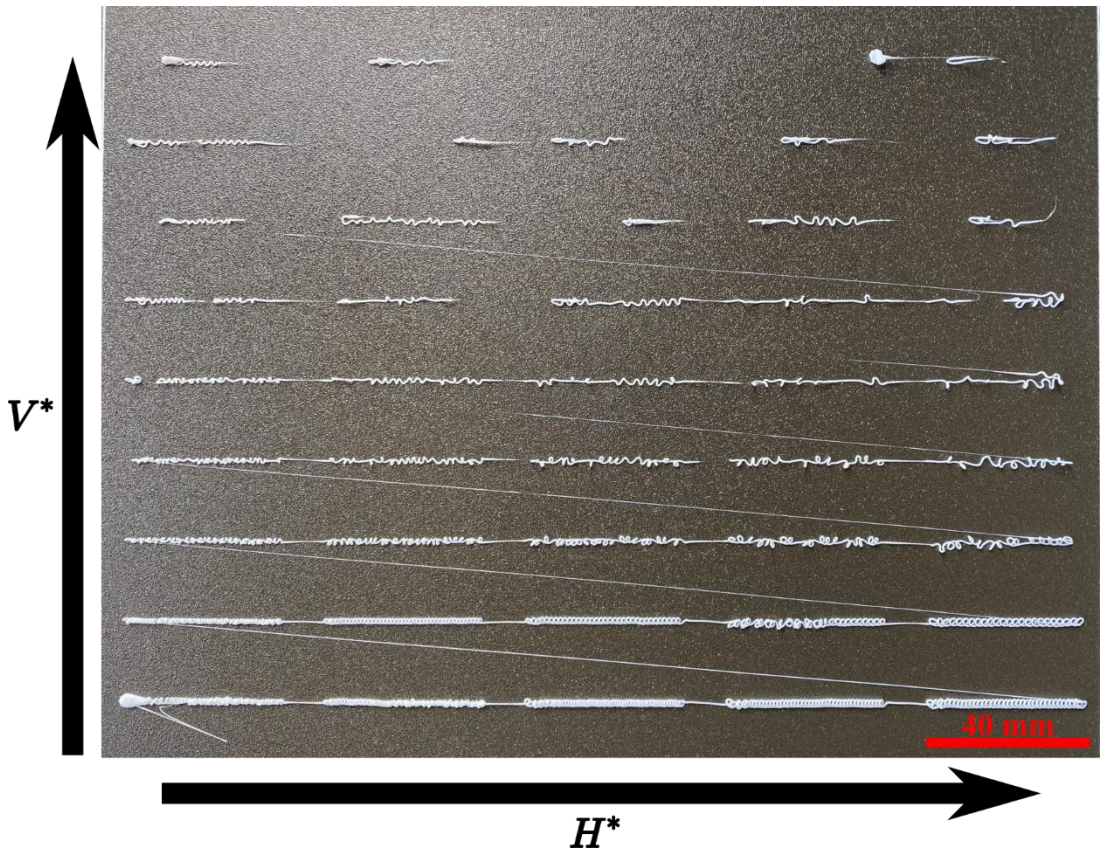


**Figure 1** - V*/H* sweep from 0.1-1 and 5-10 respectively

accumulation and for H* > 10 the TPU had difficultly sticking to the build plate for many V* values greater than 0.45 making regular coiling difficult to control.

For characterization in 2D, coil meshes are formed by continuously extruding material in a zig-zagging toolpath pattern as seen in **Figure 2**. The length of any side of the zigzag is defined as L, while the spacing between continuous L moves is λ. In this case L defines the overall geometry but λ contributes directly to the density of the mesh in addition to the consistency of coiling. λ must be empirically determined so that the coiling behavior can be properly controlled to ensure good overlap between passes of coils while also programming the density of the mesh. In all, the translation from 1D to 2D coiling behavior is straightforward with the major exception that as coils begin to overlap the resulting new coil becomes unstable and unpredictable. For any isolated 1D line the coiling behavior will reach a metastable state that can easily be perturbed by a non-uniform build surface or a change in velocity. Once perturbed, the coiling behavior will be temporarily destabilized until the printed line is no longer being influenced and is allowed to reestablish its metastable state.

**3D Characterization**

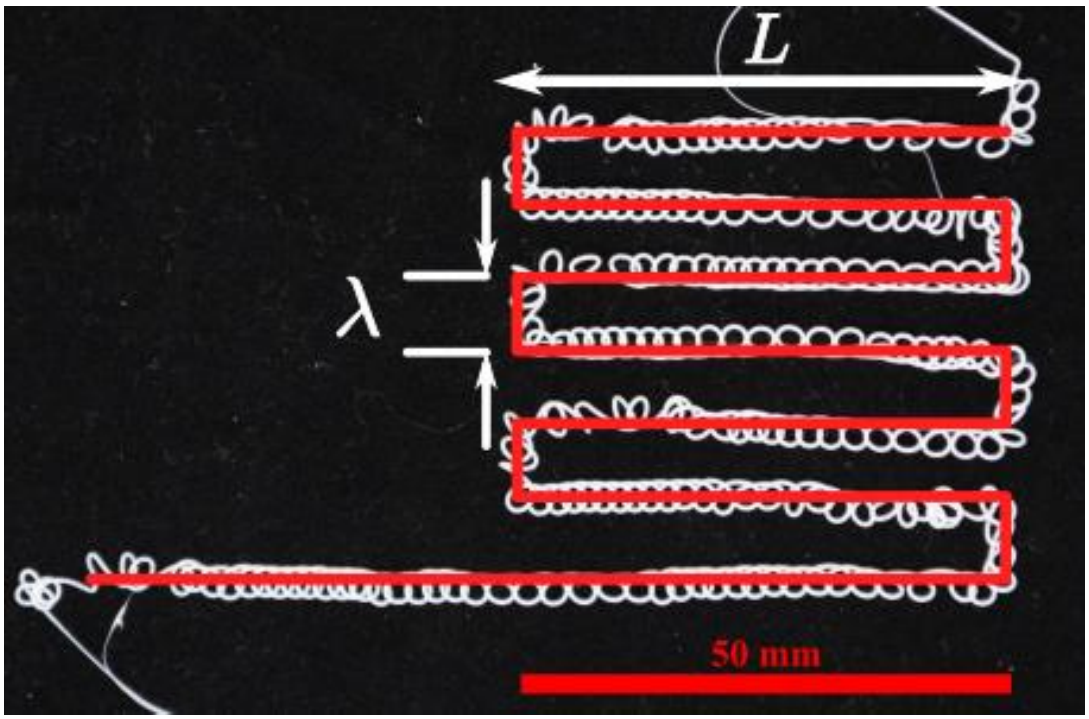


**Figure 2** - Zigzag toolpath pattern to produce a 2D mesh

In order to achieve a well-formed cube, the parameters V*, H* and λ are tuned to program the density for a one-layer mesh. The single layer thickness Δz is then measured by hand to determine the necessary z-axis increment to build successive mesh layers on top of each other to achieve the desired density 3D foam cube. This is affected by many factors such as how much parallel coils overlap, how much the loops of a coil overlaps with the next, and how flat the build surface is. A constant Δz is used to achieve an approximately constant H* value at a given layer to maintain as consistent of a coiling pattern as possible. The zig zag pattern is then rotated for each layer by 90$^{o}$ resulting in a crosshatch toolpath to generate the coiled layer.

Foam homogeneity is very sensitive to the measurement of Δz. Significant non-uniformity in foam density can occur as the foam is built up even for a small error in Δz. For overestimates

of Δz, the density of the foam will decrease in the vertical direction. This is due to the increasing effective H* as the nozzle height above the foam is increasing resulting in lower frequency coiling, fewer coil overlaps, and lower layer density. Underestimating Δz will result in accumulation as the distance between nozzle and foam will continually decrease, shrinking H*, and increasing the density of the foam in the vertical direction. A properly calibrated Δz will result in a part that is nearly homogeneous, properly proportioned, and the correct height.

There are two methods of varying foam density: varying the V*,H* combination or sweeping λ. Controlling V* and H* allow for precise control of coil behavior and frequency; however, manipulation of these variables requires recalibration of λ and Δz to achieve a well-formed cube and specific density. This means that while a range of acceptable densities is achievable through direct V* and H* manipulation, at this time it is very difficult to specify a density without many trial and error experiments. The second method of programming foam density is by varying λ. As λ is swept it goes from producing significant overlap of coils to significant "dead space" between coils for a constant V*,H* combination. There is an inverse relationship between density and λ and so density can be targeted with better precision; however, for very small λ there is so much accumulation of coils on top of each other that a layer can fused into a single continuous printed piece without coiling behavior. For a very large λ relative to coil diameter the coils operate more as a loose scaffolding pattern than an open-cell foam structure.

As a rule, the density of foam is directly proportional to the quality of fine details and sharp edges. Foams with relative densities 20% or lower tend to lose their shape and have rounded features, where foams with relative densities >50% begin to have significant accumulation issues. **Figure 3** shows four small cubes printed at increasing density from left to right. The foam on the left was produced with very large coils to achieve a low density and so lacks the fine corners seen in other cubes. Conversely, the foam on the right was printed with such a small λ that accumulation caused high intra-layer adhesion and extremely poor inter-layer adhesion so that successive layers did not stick to each other well and result in an "onion" effect where layers peel apart easily. While the feature resolution of this geometry is very good, it clearly does not operate as a foam.

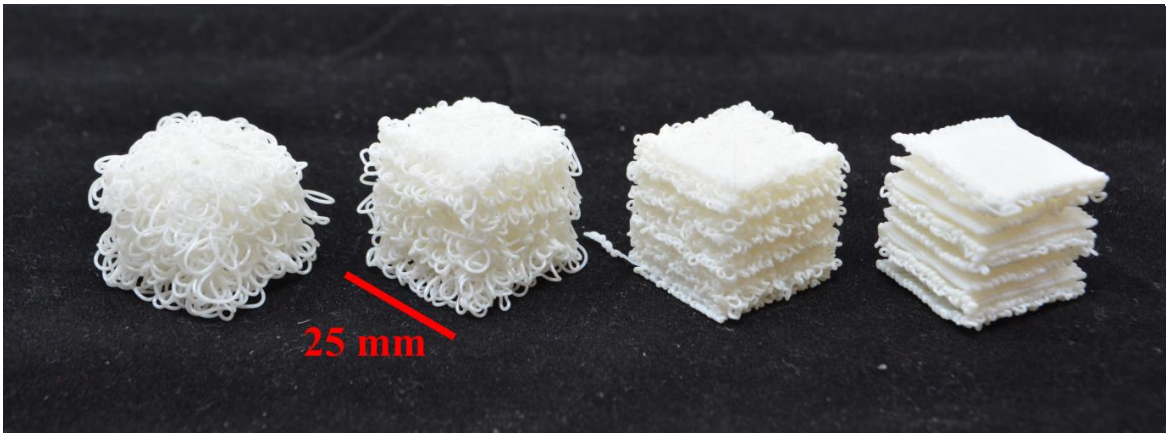


**Figure 3** - Increasing density foams approximately 15%, 25%, 40%, and 60% left to right respectively

## Results and Discussion

### Specimen Fabrication & Test

The filament used for all trials was NinjaTek NinjaFlex TPU (85A) with a density of 1.19 g/cc and a measured a die-swell (α) of 1.18. All specimens were printed at a nozzle temperature of 235°C with a build plate temperature of 40°C, and a feed rate (F) of 60 mm/min. Each specimen was printed in a cubic formfactor with nominal measurements of 50x50x50 $mm^3$. For every unique set of parameters, two specimens were printed to test the both the vertical and horizontal mechanical properties of each specimen. VTI foam specimens were prepared by varying V*/H* and/or λ at nominal densities of 15%, 25%, and 40% as outlined in **Table 1**. Cubic and grid infill specimens were printed for comparison at the same nominal densities of 15%, 25%, and 40%. These two traditional infill patterns were chosen because they are both highly prevalent in all forms of additive manufacturing and each demonstrate distinct cellular properties for our foams. Grid infill was anticipated to be highly non-uniform in stiffness along principal axes and cubic infill more uniform. All objects were printed without top or bottom layers nor walls, leaving only the inner geometry to bear all load placed upon the specimen.


**Figure 4 –** TPU foams. From left-right, top-bottom: Samples 11, 18, 19, 24 and 9.3

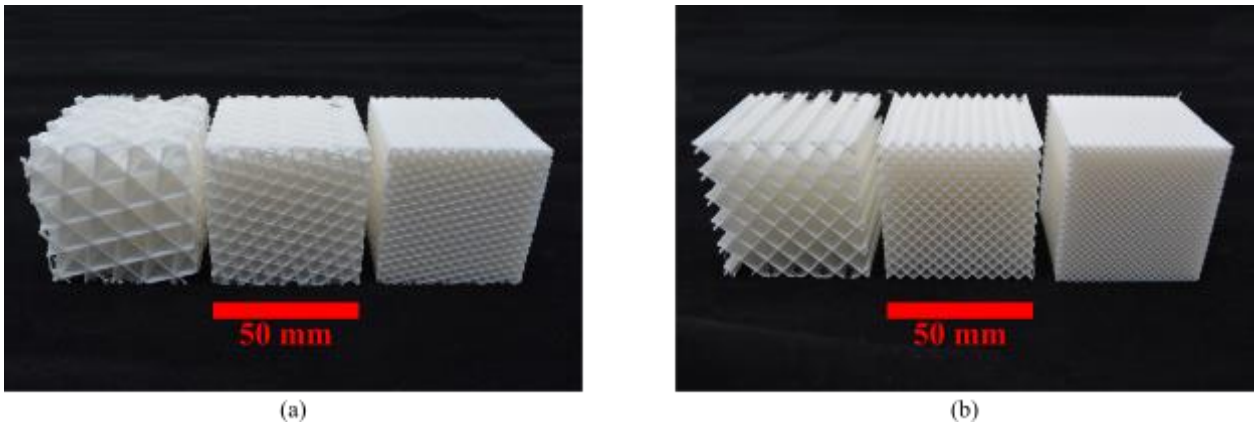


**Figure 5 -** Cubic infills (a) and grid infills (b) with nominal densities 15%, 30%, 40% from left to right in each photograph

**Table 1** - Foam fabrication variables and resulting densities normalized to TPU intrinsic density 1.19 g/cc.

| Sample No. | Nominal Density Ratio | Actual Density Ratio | V* | H* | Δz (mm) | λ (mm) |
|---|---|---|---|---|---|---|
| 24 | 15% | 12% | 0.23 | 7.5 | 0.9 | 6.5 |
| 9.3 | 15% | 18% | 0.12 | 15 | 2 | 2.5 |
| 11 | 25% | 29% | 0.23 | 7.5 | 1.3 | 1.65 |
| 18 | 25% | 24% | 0.23 | 7.5 | 1.1 | 2.5 |
| 19 | 40% | 36% | 0.23 | 7.5 | 1.2 | 1.35 |

All specimens were tested under compression vertically and horizontally as compared to original print direction. The force was applied by a 68SC-2 Instron machine, with test cell load limit of 1750N for 5 consecutive trials per specimen. Measurements were averaged together and a linear fit was determined for small strain applied in conjunction with stress as calculated by cross sectional area to determine the Young's modulus of each specimen. Density ratio was calculated as a ratio of measured density and the given manufacturer's density, where measured density was determined via measured mass over the product of measured length, width, and height of each specimen.

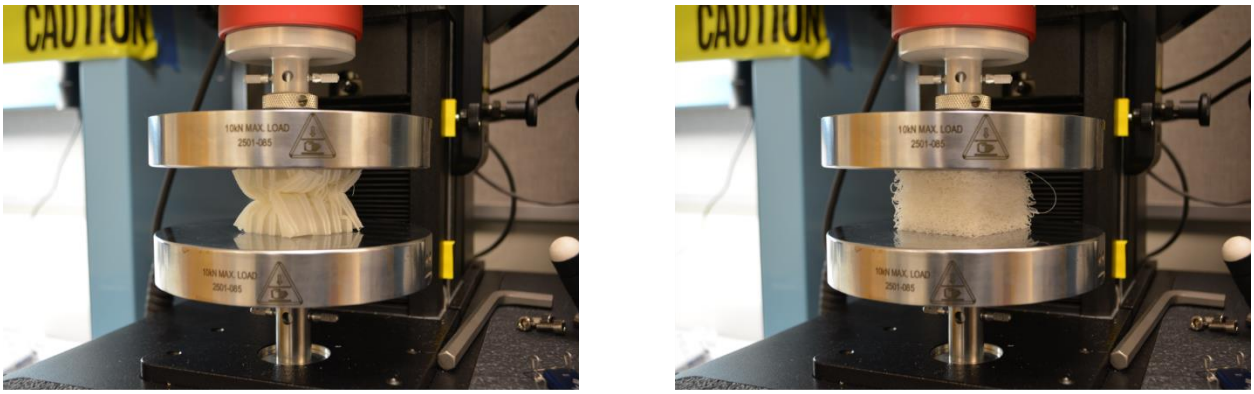


(a) (b)

**Figure 6** – (a) Vertically oriented 15% dense grid infill buckling under compression and (b) specimen number 18 under compression

## Results

**Figure 7** shows the Young's modulus of the printed foams compared to those of the printed grid and cubic infill patterns. All VTP foams can be well fit onto an exponential trendline with significantly lower Young's moduli on average than the infill specimens, with the notable exception of the horizontal grids. Tested specimens also follow a similar trend of horizontally oriented specimens generally demonstrating lower modulus values than vertically oriented specimens, likely due to the inherent layer orientation resulting from the FFF process.

The grid infill specimens were found to be highly non-uniform in stiffness along principal axes. This is due to the internal structure of grid which may be oriented to exhibit greater value of Young's modulus when vertically orientated as opposed to the significantly lower modulus of the horizontal orientation. When vertical the open cells of the grid form a very stiff structure that exhibit a greater Young's modulus than any other geometry of similar density; this trend continued for all other densities tested. This structure would behave in two distinct phases of deformation, prior to buckling and after buckling. Prior to buckling, the deformation resulting from load would

be distributed evenly over the entire structure. The original structure will be mostly maintained until a critical force is reached, at which point the structure will buckle and fold inward as seen in **Figure 6(a)**. From this point on, the specimen's stiffness would significantly decrease until densification. When horizontally oriented, grid exhibited values of Young's modulus that were significantly lower than any other infill pattern and was similar to values of the foams. Therefore, it can be concluded that the stiffness of grid infill is determined by density as well as orientation.

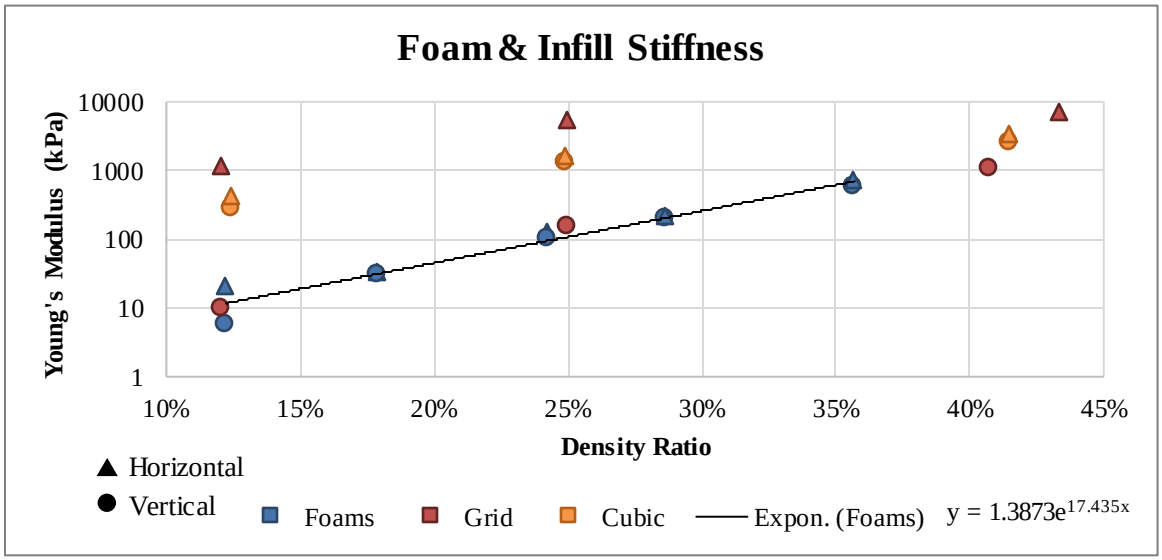


**Figure 7** - Foam and infill Young's modulus values. Grid infills tend to be highly non-uniform in stiffness along principal axes between vertical and horizontal testing, while cubic infills tend to be more uniform in stiffness along principal axes. Foam patterns also tend to be be uniform in stiffness along principal axes but with significantly lower Young's modulus as compared to the infill patterns. An exponential trendline can be drawn for the foam's with $R^2 = 0.9846$. Full values listed in **Table 2**

Cubic infill specimens were found to be highly uniform in stiffness along principal axes. This is due to the internal structure of the cubic infill being symmetrical along orthogonal axes. As such the stiffness of cubic infill specimens when vertically oriented were comparable to the stiffness of an equally dense cubic pattern when horizontally oriented. Regardless of orientation the values of Young's modulus for the cubic infills were consistently less than the values of the vertically oriented grid while also greater than the values of horizontally oriented grid and foams. While it is possible that air trapped inside the closed cellular structure could contribute to artificially high modulus values (due to compression of the air), we believe this is a negligible source due to the unlikelihood that layer adhesion of TPU is sufficiently airtight. Thus, it may be concluded that the only characteristic relevant to the stiffness of cubic infill is density.

Foams manufactured by sweeping λ as well as foams created by varying V*,H* were found to be predominantly uniform in stiffness along principal axes, where V*,H* varied foams exhibit less difference in Young's modulus than λ modulated foams. Despite this finding, generally the foams were equally uniform or better than any other geometry tested. During testing it was observed that when horizontally oriented the face composed of the first layer would deform differently than the other exposed faces. This is due to the fact that the first layer is the most well-formed of all the layers of the foam since its build area was the most flat and consistent. This results in a greater stiffness than other layers, and therefore this layer will buckle where other faces will expand uniformly outwards. As seen in **Figure 7** all tested foams can be well fit onto an

exponential trendline. The goodness of this fit can be best approximated by the $R^2$ value of 0.98. Therefore, we believe this fit very closely approximates the trend at which all foams printed in this manner will follow, allowing us to use this trend to create a framework for converting density into input variables (V*, H*, and λ). From this, it can be inferred that the most significant characteristic of a printed foam's stiffness is its density.

## Conclusions

Using viscous thread printing (VTP) of thermoplastic urethane (TPU) we successfully manufactured parts that approximate the stochastic internal structure of an open-celled foam with programable stiffness using standard fused filament fabrication (FFF) equipment. These foams are customized using dimensionless variables V* and H* to define coiling behavior as well as measured variables λ and Δz to calibrate a homogeneous internal geometry. By modulating V* and H* or by modulating λ, the densities of these foams may be tailored to many potential needs or scenarios; however, when calibrating λ or Δz both variables will affect the overall density of the resulting part. Therefore, a balance must be reached between accuracy of detail and accuracy of density. The stiffness of each specimen was determined according to deformation under load. While under such load, our foams were shown to be highly uniform in stiffness along principal axes and followed an exponential Young's modulus trend with respect to density, allowing engineering specific stiffness through simple control of the input parameters. By comparing our foams to conventional infill patterns, we have shown that our foams possess pic properties similar to cubic infill along principal axes with stiffness most similar to horizontally oriented grid infill. As such our foams fill a unique niche leveraging the properties of some infill patterns while balancing their disadvantages where no standard infill can achieve both simultaneously.

## Acknowledgements

This work was made possible by a gift from the Ford Motor Company as well as by a grant from the NASA Space Grant Initiative and scholarship support from the Mary Gates Endowment. We thank the Murdock Charitable Trust, for their support through grant 201913596.

## References


1. Derby B. Printing and prototyping of tissues and scaffolds. Science. 2012;338: 921–926.

2. Melchels FPW, Domingos MAN, Klein TJ, Malda J, Bartolo PJ, Hutmacher DW. Additive manufacturing of tissues and organs. Prog Polym Sci. 2012;37: 1079–1104.

3. Chu C, Graf G, Rosen DW. Design for additive manufacturing of cellular structures. Comput Aided Des Appl. 2008. Available: https://www.tandfonline.com/doi/abs/10.3722/cadaps.2008.686-696

4. Gibson I, Rosen D, Stucker B, Khorasani M. Design for additive manufacturing. Additive manufacturing. 2021. Available: https://link.springer.com/chapter/10.1007/978-3-030-56127-7_19

5. Murr LE, Gaytan SM, Medina F, Martinez E, Martinez JL, Hernandez DH, et al. Characterization of Ti–6Al–4V open cellular foams fabricated by additive manufacturing using electron beam melting. Mater Sci Eng A Struct Mater. 2010;527: 1861–1868.

6. Bauer J, Hengsbach S, Tesari I, Schwaiger R, Kraft O. High-strength cellular ceramic composites with 3D microarchitecture. Proc Natl Acad Sci U S A. 2014;111: 2453–2458.

7. Nguyen J, Park S-I, Rosen D. Heuristic optimization method for cellular structure design of light weight components. International Journal of Precision Engineering and Manufacturing. 2013;14: 1071–1078.

8. Cheng L, Zhang P, Biyikli E, Bai J, Pilz S, To AC. Integration of topology optimization with efficient design of additive manufactured cellular structures. Solid Freeform Fabrication Symposium (SFF), Austin, TX, Aug. utw10945.utweb.utexas.edu; 2015. pp. 10–12.

9. Cheng L, Zhang P, Biyikli E, Bai J, Robbins J, To A. Efficient design optimization of variable-density cellular structures for additive manufacturing: theory and experimental validation. &ctx_ver=Z. 2017;39: 88.

10. Gibson I, Rosen D, Stucker B, Khorasani M. Additive manufacturing technologies. Springer. Available: https://link.springer.com/content/pdf/10.1007/978-3-030-56127-7.pdf

11. Lipton JI, Lipson H. 3D Printing Variable Stiffness Foams Using Viscous Thread Instability. Sci Rep. 2016;6: 29996.

12. Morris SW, Dawes JHP, Ribe NM, Lister JR. Meandering instability of a viscous thread. Phys Rev E Stat Nonlin Soft Matter Phys. 2008;77: 066218.

13. Brun P-T, Audoly B, Ribe NM, Eaves TS, Lister JR. Liquid ropes: a geometrical model for thin viscous jet instabilities. Phys Rev Lett. 2015;114: 174501.

14. Srivastava S, Driessen T, Jeurissen R, Wijshoff H, Toschi F. Lattice Boltzmann method to study the contraction of a viscous ligament. arXiv [physics.flu-dyn]. 2013. Available: http://arxiv.org/abs/1305.6189

15. Yuk H, Zhao X. A New 3D Printing Strategy by Harnessing Deformation, Instability, and Fracture of Viscoelastic Inks. Adv Mater. 2018;30. doi:10.1002/adma.201704028

# Supplemental

**Table 2** - Printed specimen results

| Sample No. | Actual Density Ratio | Test Orientation | L (mm) | W (mm) | H (mm) | Young's Modulus (kPa) |
|---|---|---|---|---|---|---|
| 24 | 12% | V | 51.7 | 51.7 | 48 | 20.12 |
| 24 | 12% | H | 51.7 | 51.7 | 48 | 5.72 |
| 9.3 | 18% | V | 50 | 50 | 46 | 32.91 |
| 9.3 | 18% | H | 50 | 50 | 46 | 31.05 |
| 11 | 29% | V | 50 | 50 | 49.5 | 193.89 |
| 11 | 29% | H | 50 | 50 | 49.5 | 216.54 |
| 18 | 24% | V | 50 | 50 | 49.7 | 124.63 |
| 18 | 24% | H | 50 | 50 | 49.7 | 98.36 |
| 19 | 36% | V | 52 | 52 | 51.5 | 589.58 |
| 19 | 36% | H | 52 | 52 | 51.5 | 708.52 |
| Grid 15% | 12% | V | 48.7 | 48.7 | 50.2 | 1098.86 |
| Grid 15% | 12% | H | 48.7 | 48.7 | 50.2 | 9.71 |
| Grid 30% | 25% | V | 49.2 | 49.2 | 50.3 | 5147.30 |
| Grid 30% | 25% | H | 49.2 | 49.2 | 50.3 | 152.85 |
| Grid 50% | 43% | V | 49.65 | 49.65 | 50.2 | 7070.19 |
| Grid 50% | 41% | H | 49.65 | 49.65 | 50.2 | 1069.00 |
| Cubic 15% | 12% | V | 49.6 | 49.6 | 50 | 285.38 |
| Cubic 15% | 12% | H | 49.6 | 49.6 | 50 | 403.98 |
| Cubic 30% | 25% | V | 49.7 | 49.7 | 50.3 | 1311.05 |
| Cubic 30% | 25% | H | 49.7 | 49.7 | 50.3 | 1548.73 |
| Cubic 50% | 41% | V | 49.65 | 49.65 | 50.3 | 2591.12 |
| Cubic 50% | 41% | H | 49.65 | 49.65 | 50.3 | 3261.43 |